PHYSICAL REVIEW B **89**, 165429 (2014)

Modes and resonances of plasmonic scatterers

Jouni Mäkitalo* and Martti Kauranen
Department of Physics, Tampere University of Technology, P.O. Box 692, FI-33101 Tampere, Finland

Saku Suuriniemi
Department of Electrical Engineering, Tampere University of Technology, P.O. Box 692, FI-33101 Tampere, Finland
(Received 7 November 2013; revised manuscript received 14 April 2014; published 29 April 2014)

We present a rigorous full-wave electromagnetic approach to analyze the modes and resonances of dielectric and plasmonic nanoparticles of practically any geometry. Using boundary integral operators, we identify the resonances as inherent properties of the particles and propose a modal expansion for their optical response. We show that the resonance frequencies are isolated points on the complex plane. The approach allows the particles to be analyzed without specifying an incident field, which can be separately tailored for the desired interaction with the modes. We also connect the general theory to the Mie theory in spherical geometry and provide a connection to the quasistatic theory. In comparison to earlier work on modes and resonances of scatterers, our approach has the benefit that modes are defined entirely over a compact boundary surface of the scatterer. Furthermore, the boundary integral operator is of second-kind Fredholm type, enabling the rigorous characterization of the resonances.

DOI: 10.1103/PhysRevB.89.165429 PACS number(s): 42.25.Fx, 02.30.Rz, 02.30.Sa, 73.20.Mf

I. INTRODUCTION

The optical responses of metal nanoparticles arise from the collective oscillations of their conduction electrons [1]. The responses are often discussed in terms of plasmon resonances and modes, which give rise to enhanced local fields near the particle surface, thereby amplifying optical processes, such as Raman scattering [2] and second-harmonic generation [3]. The resonances can be broadly tuned for a given application by the size, shape, and dielectric environment of the particles [4]. The concepts of mode and resonance are routinely used to describe conventional optical systems, such as cavities and waveguides, where the electromagnetic fields are defined within bounded domains. Mathematically, such problems are described by a self-adjoint Helmholtz operator, whose corresponding integral operator is compact, leading to a discrete modal eigenbasis, directly related to the resonances of the system. Such characterization of the operator spectrum is a central problem in the study of resonances.

In contrast, the electromagnetic interaction with nanoparticles is essentially a scattering problem, defined over an unbounded spatial domain. This makes it, mathematically speaking, difficult to characterize the spectrum of the pertinent operator and thus to define the resonances of the particle. Furthermore, it is not clear whether the resonances can be associated with any well-defined electromagnetic eigenmodes. For plasmonic metal nanoparticles, the casual use of the concept of resonance thus only implies that the plasmonic responses become strong at certain frequencies. This is commonly analyzed by relying on an incident probe field, usually a plane wave. The resulting near-field patterns are then qualitatively classified as modes. This approach depends on the chosen incident field and may not find all resonances, e.g., ones related to dark modes [5]. Neither does the approach reveal whether the field patterns are due to a single discrete mode, a combination of modes, or possibly a continuum of modes. Especially in the plasmonic community, previous approaches to resonances and modes have been by and large restricted to microscopic electron oscillation formalism [6,7] or perturbation of macroscopic electric fields based on quasistatics [8–12], only valid for scatterers much smaller than wavelength. These approaches do not fully account for radiation, i.e., time-dependent effects, which are very important for many common nanosystems, especially large particles.

Beyond the quasistatic regime, modes and resonances have been considered by various approaches in other branches of physics. One of the earliest theoretical works was by Baum on the identification of perfectly conducting targets by electromagnetic pulses relying on integral operators [13]. This, so-called singularity expansion method, was complemented by another approach, based on so-called characteristic modes (eigenmodes) of conducting objects [14]. This work was further developed in [15,16], and the theory has found applications in, e.g., evaluating antenna quality factors independent of excitation [17]. Some studies based on the volume integral operator have been done for dielectric [18–20] and plasmonic [21–23] objects. The volume integral operator involves a strongly singular kernel, which complicates the characterization of the operator spectrum and thus the physical resonances [24–26].

Further approaches include a coupled-dipole description [27], inverse scattering matrix analysis in the Fourier modal method [28,29], and modal solution of the Maxwell differential equations [30,31]. Little to no spectral analysis was presented in these cases.

Recently, the boundary integral operators have been found powerful in the accurate modeling of the linear [32–35] and nonlinear [36] optical properties of plasmonic nanoparticles. Boundary integral operators have been utilized for analyzing the resonances of two-dimensional dielectric bodies [37] and the eigenmodes of three-dimensional dielectric objects [38]. On the other hand, there has been increased interest in

*jouni.makitalo@tut.fi

discovering modal expansions for plasmonic scattering problems, as this enables a meaningful approach to the evaluation of mode volumes and the Purcell factor [39,40]. This factor is proportional to the partial local density of states (LDOS), which determines the spontaneous emission decay rate of a dipole emitter [41]. The modes of the system determine the LDOS, which is then a measurable quantity that is independent of excitation. Thus a theoretically sound approach to modes and resonances by boundary integral operators is called for.

In this paper, we present an approach that allows the modes and resonances of essentially arbitrary nanoparticles to be analyzed in the strict electromagnetic sense, fully accounting for radiation effects. The approach treats the modes and resonances as inherent properties of the particle itself, independent of any incident field. By relying on boundary integral operators, the modes are defined over the spatially bounded surface of the particle and can be related to its resonances. We further show that our approach is compatible with the Mie theory for spherical particles and show calculations for more complicated shapes. By separating the particle properties from the incident field, our approach can provide fundamental information on very general nanoparticle systems. Our approach is applicable to particles made of any piecewise homogeneous material. However, it has particular importance in plasmonics, where the applications are based on detailed tailoring of the near field at the particle surface.

II. BOUNDARY INTEGRAL OPERATORS

Our rigorous electromagnetic approach to modes and resonances in scattering problems is based on a boundary integral formulation, where the modes are defined over the surface of the nanoparticle. The particle occupies a bounded domain V_2 with complex permittivity ϵ_2 and permeability μ_2 as illustrated in Fig. 1. The domain V_1, external to V_2, is unbounded with real permittivity ϵ_1 and permeability μ_1. The particle surface S is assumed C^2 smooth, i.e., a normal $\mathbf{n}$ pointing into V_1 exists at each point on S and varies continuously.

First we consider the direct scattering problem, where incident fields $\mathbf{E}_{\text{inc}}$ and $\mathbf{H}_{\text{inc}}$ are known and the electric fields $\mathbf{E}_l$ and magnetic fields $\mathbf{H}_l$ over domains V_l ($l = 1,2$) are sought. The fields have complex time-harmonic dependence $\exp(-i\omega t)$, satisfy the vector Helmholtz equations [42] in V_1 and V_2, and have tangential continuity on S. The scattered fields $\mathbf{E}_s = \mathbf{E}_1 - \mathbf{E}_{\text{inc}}$ and $\mathbf{H}_s = \mathbf{H}_1 - \mathbf{H}_{\text{inc}}$ must be outwards

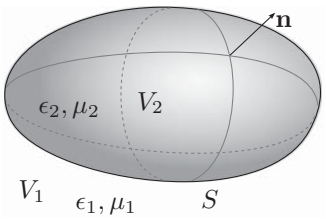

FIG. 1. Prototype geometry and parameters of the scattering problem.

propagating transverse spherical waves far from the particle,

$$\lim_{|\mathbf{r}|\to\infty} \sqrt{\epsilon_1}\mathbf{E}_s \times \mathbf{r} + |\mathbf{r}|\sqrt{\mu_1}\mathbf{H}_s = \mathbf{0}, \tag{1}$$

which is called the Silver-Müller radiation condition. This condition is sufficient to determine a unique solution to the Helmholtz equations with given incident fields. However, the condition renders the Helmholtz operators non-self-adjoint. Furthermore, because the solution domain is unbounded, it is difficult to analyze the modes and resonances using the Helmholtz operator. Specifically, the fields involved are not square-integrable over V_1, as an infinite amount of energy has been scattered in the steady state.

We avoid these issues by reformulating the problem using integral operators, which bring the problem to the compact (bounded and closed) surface S. This is done by introducing the fundamental Green's function $G_l(\mathbf{r},\mathbf{r}') = \exp(ik_l R)/(4\pi R)$ ($R = |\mathbf{r} - \mathbf{r}'|$) for the two domains $l = 1,2$ with wave numbers $k_l = \omega\sqrt{\epsilon_l \mu_l}$. We define boundary integral operators, which map functions $\mathbf{f} : \partial V_l \to \mathbb{C}^3$ defined over the surface to functions defined over the domains V_l:

$$(\mathcal{D}_l\mathbf{f})(\mathbf{r}) = i\omega\mu_l \int_{\partial V_l} G_l(\mathbf{r},\mathbf{r}')\mathbf{f}(\mathbf{r}')dS' - \frac{1}{i\omega\epsilon_l}\nabla \int_{\partial V_l} G_l(\mathbf{r},\mathbf{r}')\nabla'_t \cdot \mathbf{f}(\mathbf{r}')dS', \tag{2}$$

$$(\mathcal{K}_l\mathbf{f})(\mathbf{r}) = \int_{\partial V_l} [\nabla' G_l(\mathbf{r},\mathbf{r}')] \times \mathbf{f}(\mathbf{r}')dS', \tag{3}$$

where $\nabla_t \cdot \mathbf{f}$ is the surface (tangential) divergence.

Through the use of Green's function and Green's identities we may derive the so-called Stratton-Chu equations [42], which give the fields over V_1 and V_2 from functions on S through the integral operators:

$$\Omega_l\mathbf{H}_l = \delta_{l1}\mathbf{H}_{\text{inc}} + \mathcal{D}_l\mathbf{E}_l \times \mathbf{n}_l/\eta_l^2 - \mathcal{K}_l\mathbf{n}_l \times \mathbf{H}_l, \tag{4}$$

$$\Omega_l\mathbf{E}_l = \delta_{l1}\mathbf{E}_{\text{inc}} + \mathcal{D}_l\mathbf{n}_l \times \mathbf{H}_l + \mathcal{K}_l\mathbf{E}_l \times \mathbf{n}_l, \tag{5}$$

where normals $\mathbf{n}_l$ point into V_l and we introduced the impedance $\eta_l = \sqrt{\mu_l/\epsilon_l}$ and the Kronecker delta, δ_{nm}. The number Ω_l equals 1 if $\mathbf{r} \in V_l - \partial V_l$, zero if $\mathbf{r} \notin V_l \cup \partial V_l$, and $1/2$ if $\mathbf{r} \in \partial V_l$. The scattered fields given by the operators satisfy the Silver-Müller conditions. The operators $\mathcal{D}_l$, however, have strongly singular kernels due to the gradient term, which makes the analysis of modes and resonances more challenging.

It is conventional to introduce the equivalent surface current densities to represent the boundary fields:

$$\mathbf{J}_l = \mathbf{n}_l \times \mathbf{H}_l, \tag{6}$$

$$\mathbf{M}_l = \mathbf{E}_l \times \mathbf{n}_l. \tag{7}$$

In terms of these quantities, we obtain the following boundary integral equations:

$$\tfrac{1}{2}\mathbf{J}_l = \delta_{l1}\mathbf{J}_{\text{inc}} + \mathbf{n}_l \times \mathcal{D}_l\mathbf{M}_l/\eta_l^2 - \mathbf{n}_l \times \mathcal{K}_l\mathbf{J}_l, \tag{8}$$

$$\tfrac{1}{2}\mathbf{M}_l = \delta_{l1}\mathbf{M}_{\text{inc}} - \mathbf{n}_l \times \mathcal{D}_l\mathbf{J}_l - \mathbf{n}_l \times \mathcal{K}_l\mathbf{M}_l, \tag{9}$$

where the integration in $\mathcal{K}_l$ is defined in the Cauchy principal value sense [42].

There are various ways to formulate the scattering problem by the use of the Eqs. (8) and (9). However, in the Müller formulation [43], the strong singularities in the operators $\mathcal{D}_l$ cancel out, enabling us to rigorously analyze the physical resonances. Next we derive this formulation. Let $\xi_\epsilon = 1/(\epsilon_1 + \epsilon_2)$ and $\xi_\mu = 1/(\mu_1 + \mu_2)$. Then multiply Eq. (8) by $\mu_l \xi_\mu$ and Eq. (9) by $\epsilon_l \xi_\epsilon$ and subtract the equations corresponding to the two domains. Further, we impose the continuity of the tangential field components as

$$\mathbf{J} = \mathbf{J}_1 = -\mathbf{J}_2, \tag{10}$$

$$\mathbf{M} = \mathbf{M}_1 = -\mathbf{M}_2, \tag{11}$$

and set $\mathbf{n} = \mathbf{n}_1 = -\mathbf{n}_2$ to obtain [43,44]

$$\begin{aligned}\tfrac{1}{2}\mathbf{J} = \xi_\mu[&\mu_1 \mathbf{J}_{\text{inc}} + (\epsilon_1 \mathbf{n}\times\mathcal{D}_1 - \epsilon_2 \mathbf{n}\times\mathcal{D}_2)\mathbf{M} \\ &+ (-\mu_1 \mathbf{n}\times\mathcal{K}_1 + \mu_2 \mathbf{n}\times\mathcal{K}_2)\mathbf{J}],\end{aligned} \tag{12}$$

$$\begin{aligned}\tfrac{1}{2}\mathbf{M} = \xi_\epsilon[&\epsilon_1 \mathbf{M}_{\text{inc}} + (-\epsilon_1 \mathbf{n}\times\mathcal{D}_1 + \epsilon_2 \mathbf{n}\times\mathcal{D}_2)\mathbf{J} \\ &+ (-\epsilon_1 \mathbf{n}\times\mathcal{K}_1 + \epsilon_2 \mathbf{n}\times\mathcal{K}_2)\mathbf{M}].\end{aligned} \tag{13}$$

This can be arranged into a matrix form,

$$(\mathcal{I} + \mathcal{A}(\omega))\mathbf{f} = \mathbf{g}, \tag{14}$$

where $\mathcal{I}$ is the identity operator, $\mathbf{f} = (\eta_1 \mathbf{J}, \mathbf{M})$ is the unknown solution, and $\mathbf{g} = (2\eta_1\mu_1\xi_\mu \mathbf{J}_{\text{inc}}, 2\epsilon_1\xi_\epsilon \mathbf{M}_{\text{inc}})$ is the tangential component of the incident field on S and the matrix entries can be deduced directly from Eqs. (12) and (13). We write the frequency dependency of the operator $\mathcal{A}(\omega)$ explicitly as we are interested in the resonance frequencies.

III. ANALYSIS OF BOUNDARY INTEGRAL OPERATORS

In this section we review some results of functional analysis of linear operators between Hilbert spaces. In the spectral analysis, the concepts of adjoint operator and compact operator are paramount. We denote by $L^2(S)$ a Hilbert space of square-integrable functions over a surface S endowed with an inner product $\langle\cdot,\cdot\rangle$. The *adjoint* of an operator $\mathcal{L} : L^2(S) \to L^2(S)$, denoted by $\mathcal{L}^\dagger$, satisfies $\langle \mathcal{L}\mathbf{f}_1, \mathbf{f}_2\rangle = \langle \mathbf{f}_1, \mathcal{L}^\dagger \mathbf{f}_2\rangle$ for all $\mathbf{f}_1$ and $\mathbf{f}_2$ in $L^2(S)$. A particularly well-studied class of operators are the self-adjoint operators, for which $\mathcal{L} = \mathcal{L}^\dagger$ holds.

The inner product induces the norm $|\mathbf{f}| = \sqrt{\langle \mathbf{f}, \mathbf{f}\rangle}$. An operator $\mathcal{L}$ is *bounded* if there exists a positive real number K such that $|\mathcal{L}\mathbf{f}| < K|\mathbf{f}|$ for all $\mathbf{f}$. Bounded operators always have a unique adjoint. A bounded operator is *compact*, if for every sequence in the domain of the operator there exists a convergent subsequence in the image sequence. The intuition behind a compact operator $\mathcal{L}$ is that there exists a finite-dimensional subspace M of the range of $\mathcal{L}$ such that any image $\mathcal{L}\mathbf{f}$ can be approximated to an arbitrary degree by an element of M. Thus compact operators are among the best-understood operators mapping between infinite-dimensional spaces.

The spectrum of an operator $\mathcal{L}$ is defined in terms of the resolvent operator $(\mathcal{L} - \lambda\mathcal{I})^{-1}$ [45]. The complex numbers λ are generally divided into two disjoint subsets: *the spectrum* $\sigma(\mathcal{L})$ and *the resolvent set* $\rho(\mathcal{L}) = \mathbb{C} - \sigma(\mathcal{L})$. A number λ is defined to be in the spectrum $\sigma(\mathcal{L})$, if the resolvent fails to exist as a bounded operator for this number. Otherwise the number λ is said to be in the resolvent set $\rho(\mathcal{L})$. The spectrum can be further decomposed into disjoint sets called the point spectrum (the eigenvalues), the continuous spectrum, and the residual spectrum. Finding these sets is a central problem in the spectral theory of linear operators.

An important property of compact operators is that all nonzero spectral values are eigenvalues [45]. Furthermore, their point spectrum is discrete (despite the name, the point spectrum of an operator is not a discrete set in general) and the elements may be arranged so that they tend towards zero. Operators of the form $\mathcal{I} + \mathcal{L}$, where $\mathcal{L}$ is compact, are called *Fredholm operators of the second kind* [45]. For such operators, resonances can be rigorously identified and this is done in the next section.

We next consider the compactness of the operators $\mathcal{D}_l$ and $\mathcal{K}_l$. Consider a surface integral operator $\mathcal{L}$ of the form

$$(\mathcal{L}f)(\mathbf{r}) = \int_S g(\mathbf{r},\mathbf{r}') f(\mathbf{r}') dS', \tag{15}$$

which maps functions defined on an n-dimensional surface S embedded in $n+1$-dimensional Euclidean space. Such an operator is compact in $L^2(S)$, if the kernel g is of the form

$$g(\mathbf{r},\mathbf{r}') = \frac{g_b(R)}{R^m}, \quad R = |\mathbf{r} - \mathbf{r}'|, \tag{16}$$

with $0 \leqslant m < n$ and g_b is bounded [45]. In our case $n = 2$ holds.

In the electromagnetic scattering problem, we come across three different kinds of integral operators involving the kernel $G(\mathbf{r},\mathbf{r}') = \exp(ikR)/(4\pi R)$. The first one is

$$(\mathcal{D}^s\mathbf{f})(\mathbf{r}) = \int_S G(\mathbf{r},\mathbf{r}')\mathbf{f}(\mathbf{r}') dS'. \tag{17}$$

In this case $m = 1$ holds, so $\mathcal{D}^s$ is compact in $L^2(S)$.

The second one is

$$(\mathcal{D}^h\mathbf{f})(\mathbf{r}) = \nabla \int_S G(\mathbf{r},\mathbf{r}')\nabla'_t \cdot \mathbf{f}(\mathbf{r}') dS'. \tag{18}$$

The kernel is hypersingular (when the gradient is moved under the integral) and the operator is noncompact, even for smooth S. Thus the characterization of the spectrum of this operator is difficult. However, in the Müller formulation, this operator only appears as differences of the form $\mathcal{D}^h_1 - \mathcal{D}^h_2$. The kernel of the operator

$$\mathcal{D}^h_1 - \mathcal{D}^h_2 = \int_S G_d(\mathbf{r},\mathbf{r}')\nabla'_S \cdot \mathbf{f}(\mathbf{r}') dS' \tag{19}$$

is

$$G_d(\mathbf{r},\mathbf{r}') = \frac{1}{4\pi}\sum_{n=0}^{\infty}\frac{n-1}{n!} R^{n-3}[(ik_1)^n - (ik_2)^n](\mathbf{r} - \mathbf{r}'), \tag{20}$$

whose first nonzero element is $n = 2$ [44]. This term is of the form $(\mathbf{r} - \mathbf{r}')/R$, whence the operator is compact.

The third operator is of the form

$$(\mathbf{n}\times\mathcal{K}\mathbf{f})(\mathbf{r}) = \mathbf{n}\times\int_S \nabla' G(\mathbf{r},\mathbf{r}')\times\mathbf{f}(\mathbf{r}') dS', \tag{21}$$

which is compact, provided that the surface is C^2 smooth [45]. The tangential trace $\mathbf{n}\times$ lowers the degree of the strong singularity in $\nabla' G$.

The domain and range of the operator $\mathcal{A}$ in the Müller formulation may be chosen as the Hilbert space of square-integrable functions embedded with the inner product

$$\langle \mathbf{f}_1, \mathbf{f}_2 \rangle = \int_S \mathbf{f}_1^* \cdot \mathbf{f}_2 dS = \int_S \left(\eta_1^2 \mathbf{J}_1^* \cdot \mathbf{J}_2 + \mathbf{M}_1^* \cdot \mathbf{M}_2 \right) dS. \quad (22)$$

IV. RESONANCES AND MODES

A. Full-wave theory

The system must have a resonance if Eq. (14) allows a nonvanishing solution for no incident field,

$$(\mathcal{I} + \mathcal{A}(\omega))\mathbf{f}_0 = 0. \quad (23)$$

This can lead to nonzero solutions $\mathbf{f}_0$ only if the inverse operator $(\mathcal{I} + \mathcal{A}(\omega))^{-1}$ is singular at certain frequencies ω, which are generally complex. Due to the compactness of $\mathcal{A}(\omega)$ as was established in the previous section, the operator $\mathcal{I} + \mathcal{A}(\omega)$ is second-kind Fredholm and the analytic Fredholm theorem is applicable [45]. Consequently, the inverse can have only pole singularities in the region of complex frequency plane where $\mathcal{A}(\omega)$ is analytic. The poles occur at isolated points [46], yielding the complex resonance frequencies, which we denote by ω_n. At all other frequencies, the inverse exists and is analytic. The resonance modes $\mathbf{f}_{0n}$ corresponding to a given ω_n constitute a finite-dimensional space, i.e., there can be only finite degeneracy [45]. The resonance frequencies shift continuously as S changes continuously [45]. *After fixing the geometry and media, the resonances can thus be solved from Eq. (23) with no assumed incident field.*

In the near-infrared and optical regimes, the permittivity of plasmonic materials can be described by the Drude model:

$$\epsilon(\omega)/\epsilon_0 = 1 - \frac{\omega_p^2}{\omega^2 + i\gamma\omega}, \quad (24)$$

where ω_p is the plasma frequency and γ is the damping frequency [47]. This dispersion gives rise to branch-point singularities at zero frequency and at $\omega = (\pm\sqrt{4\omega_p^2 - \gamma^2} - i\gamma)/2$, which give rise to two branch cuts for $\mathcal{A}(\omega)$ that restrict the region of analyticity. The structure of the resonances is illustrated in Fig. 2. The appearance of branch-point singularities due to losses was predicted in [48].

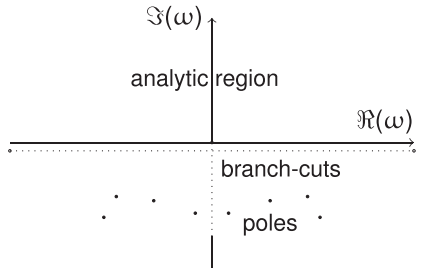

FIG. 2. Illustration of the singularities of inverse boundary integral operator for Drude-type dispersion.

Note that the resonance frequencies must reside in the lower half of the complex plane. This requirement, together with the radiation condition, implies that the scattered fields of the resonance modes $\mathbf{f}_{0n}$ grow exponentially with distance as the waves propagate towards infinity [40]. Thus, instead of using the resonance modes $\mathbf{f}_{0n}$ directly, we will look for eigenmodes defined at real frequencies to establish an expansion of solutions and relate these modes to the resonance modes found at complex frequencies.

We seek possible eigenmodes for a *fixed* real frequency ω as

$$(\mathcal{I} + \mathcal{A}(\omega))\mathbf{f}_n = \lambda_n \mathbf{f}_n, \; n \text{ integer}. \quad (25)$$

Although not explicitly indicated, these modes and eigenvalues depend also on frequency. *Thus for each fixed frequency, we obtain a set of eigenmodes*. This set is *discrete* due to the compactness [45] of $\mathcal{A}(\omega)$. It is then expected that if at a particular frequency ω there exists an eigenvalue λ_n close to zero, the corresponding mode $\mathbf{f}_n$ is nearly resonant.

We then expand the solution at frequency ω in terms of the modes

$$\mathbf{f} = \sum_n \alpha_n \mathbf{f}_n. \quad (26)$$

To relate the excitation of the modes to a given incident field $\mathbf{g}$, we need the coefficients α_n. The eigenmodes of operator $\mathcal{I} + \mathcal{A}$ are not necessarily orthogonal, as the operator $\mathcal{A}$ is not self-adjoint in general. To overcome this problem, we consider the eigenmodes of the adjoint operator $\mathcal{A}^\dagger$. If λ_n is an eigenvalue from Eq. (25) for mode $\mathbf{f}_n$, then its complex conjugate λ_n^* is an eigenvalue of the adjoint operator with corresponding adjoint mode $\mathbf{h}_n$ [45]:

$$(\mathcal{I} + \mathcal{A}^\dagger)\mathbf{h}_n = \lambda_n^* \mathbf{h}_n. \quad (27)$$

The modes and the adjoint modes are biorthogonal in the sense of $(\lambda_n - \lambda_m)\langle \mathbf{f}_n, \mathbf{h}_m \rangle = 0$ [45]. This implies $\langle \mathbf{f}_n, \mathbf{h}_m \rangle = 0$ for all $\lambda_n \neq \lambda_m$. Remember that this biorthogonality applies at a fixed frequency ω.

Through substitution of Eq. (26) to Eq. (14) and using Eq. (25), we obtain for all integers m,

$$\sum_n \alpha_n \lambda_n \langle \mathbf{h}_m, \mathbf{f}_n \rangle = \langle \mathbf{h}_m, \mathbf{g} \rangle. \quad (28)$$

Symmetries in the shape of S may lead to degenerate modes, sharing the same eigenvalue. In this case, the corresponding modes and adjoint modes are not necessarily biorthogonal, and we obtain a finite linear system for coefficients α_n. In the absence of degeneracy, we obtain

$$\alpha_n = \frac{\langle \mathbf{h}_n, \mathbf{g} \rangle}{\lambda_n \langle \mathbf{h}_n, \mathbf{f}_n \rangle}. \quad (29)$$

A small eigenvalue $|\lambda_n|$ can clearly lead to an enhanced response for the respective mode. This indicates a pole of the inverse operator at complex frequency ω_n near ω. To study the response of a particle, we first find its modes $\mathbf{f}_n$, independent of incident field, then evaluate α_n to see how a particular incident field $\mathbf{g}$ couples to the modes.

B. Quasistatic limit

The off-diagonal operators in $\mathcal{A}(\omega)$ [see Eqs. (12) and (13)] are $O(\omega)$ polynomials of frequency, even though the operators $\mathcal{D}_l$ are $O(1/\omega)$. This occurs for the same reason as the cancellation of the strong spatial singularity in the difference $\epsilon_1 \mathbf{n}\times\mathcal{D}_1 - \epsilon_2 \mathbf{n}\times\mathcal{D}_2$ [44]. For this reason, the off-diagonal operators tend to zero as ω tends to zero. This is in contrast to, e.g., the Poggio-Miller-Chang-Harrington-Wu-Tsai (PMCHWT) formulation [49], for which the zero-frequency limit does not exist due to a $1/\omega$ factor. The limit of the operator $\mathcal{K}_l$ is simply

$$\lim_{\omega\to 0}(\mathcal{K}_l\mathbf{f})(\mathbf{r}) = (K\mathbf{f})(\mathbf{r}) = \int_{\partial V_l} \nabla' \frac{1}{4\pi R} \times \mathbf{f}(\mathbf{r}')dS'. \quad (30)$$

Thus the static limit is

$$\mathcal{A}(0) = 2\begin{pmatrix} \frac{\mu_1-\mu_2}{\mu_1+\mu_2}\mathbf{n}\times K & 0 \\ 0 & \frac{\epsilon_1-\epsilon_2}{\epsilon_1+\epsilon_2}\mathbf{n}\times K \end{pmatrix}, \quad (31)$$

where the electric and magnetic parts are decoupled.

Then the electrostatic (or quasistatic) formulation is obtained via introduction of the electrostatic potential ϕ so that $\mathbf{E} = -\nabla\phi$:

$$\phi - \lambda K\phi = 2\epsilon_1\phi^{\text{inc}}, \quad (32)$$

$$(K\phi)(\mathbf{r}) = \frac{1}{2\pi}\int_S \frac{\partial}{\partial n'}\frac{1}{R}\phi(\mathbf{r}')dS', \quad (33)$$

where $\lambda = (\epsilon_2-\epsilon_1)/(\epsilon_2+\epsilon_1)$. This potential formulation has been used to define plasmon resonances in the quasistatic limit [9]. It can be shown that $|\lambda| \geqslant 1$ holds for the eigenvalues λ. This condition is only met in practice if $\Re(\epsilon_2) < 0$ holds, which is characteristic of plasmonic materials. Note that in the quasistatic regime, K is not frequency dependent, but ϵ_2 is considered frequency dependent. Thus the eigenvalue λ yields eigenpermittivity ϵ_2, which yields a resonance frequency through a dispersion relation. In the time-harmonic case, the operators depend on both $\epsilon_2(\omega)$ and ω in a nontrivial way such that the frequency dependence cannot be separated from the operators as a simple multiplication by a constant.

The theory of resonances based on the Müller formulation is then a generalization of the quasistatic theory [9]. A curious difference in the spectral structure of the full-wave and quasistatic cases can be observed: in the latter, the imaginary part of a resonance frequency is directly determined by the material damping constant γ. This is also true for all higher-order perturbation corrections, as the quasistatic eigenvalue is always real valued. Consequently, the quasistatics-based perturbation predicts that all resonance frequencies reside on the branch cut. This is not the case in general, and as we shall see in Sec. VII, the resonance frequencies reside rather far off from this branch cut, even for moderately sized nanoparticles. This further suggests that the quasistatics-based perturbation series does not converge towards a correct solution.

V. FINITE-DIMENSIONAL FORMULATION

A. Method of moments

In practice, the solution to Eqs. (23) and (25) may not be found in closed form if the geometry is complicated. To obtain approximate solutions to Eq. (14) by numerical computation, we utilize the method of moments with Galerkin's weighting [50]. The space $L^2(S)$ is approximated by a finite-dimensional space spanned by the Rao-Wilton-Glisson (RWG) functions [51]. An RWG function $\mathbf{b}_n$ is nonzero only over a pair of triangles T_n^+ and T_n^- of areas A_n^+ and A_n^- and the triangles have a common edge of length l_n. The vertices off the common edge are denoted $\mathbf{r}_n^+$ and $\mathbf{r}_n^-$. With these notations,

$$\mathbf{b}_n(\mathbf{r}) = \begin{cases} \frac{l_n}{2A_n^+}(\mathbf{r}-\mathbf{r}_n^+), & \mathbf{r}\in T_n^+ \\ \frac{l_n}{2A_n^-}(\mathbf{r}_n^- - \mathbf{r}), & \mathbf{r}\in T_n^- \\ 0, & \text{otherwise.} \end{cases} \quad (34)$$

The surface divergence of RWG functions exists over $T_n^- \cup T_n^+$ and thus the approximate space is divergence conforming.

We next seek solutions to Eq. (14) from the space spanned by the RWG functions. By the use of the method of moments, a linear system of equations is obtained. We define the following basis moment matrix:

$$B_{mn} = \int_S \mathbf{b}_m \cdot \mathbf{b}_n dS; \quad (35)$$

and the following functions:

$$\mathbf{b}'_n = \begin{cases} (\mathbf{b}_n, \mathbf{0})^T, & n = 1,2,\ldots,N \\ (\mathbf{0}, \mathbf{b}_n)^T, & n = N+1, N+2, \ldots, 2N; \end{cases} \quad (36)$$

and the following matrix:

$$\mathrm{B}' = \begin{pmatrix} \mathrm{B} & 0 \\ 0 & \mathrm{B} \end{pmatrix}. \quad (37)$$

The solution is then expanded as

$$\mathbf{f} = \sum_{n=1}^{2N} c_n \mathbf{b}'_n. \quad (38)$$

This expression is inserted into $(\mathcal{I}+\mathcal{A})\mathbf{f} = \mathbf{g}$, which is then tested by $\mathbf{b}'_m$ via the inner product $\langle\cdot,\cdot\rangle$, which results in the following linear system of equations:

$$(\mathrm{B}' + \mathrm{A})\mathbf{x} = \mathbf{y}, \quad (39)$$

where $\mathbf{x} = \{c_1, c_2, \ldots, c_{2N}\}$ and the components of $\mathbf{y}$ are $y_m = \langle \mathbf{b}'_m, \mathbf{g}\rangle$. The components of the matrix A are $A_{mn} = \langle \mathbf{b}'_m, \mathcal{A}\mathbf{b}'_n\rangle$. The linear system of equations is generally well conditioned due to the second-kind Fredholm nature of the operator [44].

The matrix elements A_{mn} involve the evaluation of integrals with weakly singular kernels. The evaluation was done by the use of the singularity subtraction technique [52], where the singular parts are integrated analytically and a seventh-order Gauss-Legendre quadrature is used for the remaining smooth part.

The off-diagonal elements of the operator A require evaluation of the expression

$$I = \int_{T_m^\pm} \mathbf{b}_m \cdot \mathbf{n}\times\nabla \int_{T_n^\pm} G_s(\mathbf{r},\mathbf{r}')\nabla'_t \cdot \mathbf{b}_n dS' dS, \quad (40)$$

where the subscripts 1 and 2 refer to the external and the particle domains, respectively. We denote a combined kernel as $G_s = G_1 - G_2$. The application of partial integration to the outer integral yields

$$I = \int_{\partial T_m^\pm} \mathbf{b}_m \cdot \mathbf{l} \int_{T_n^\pm} G_s(\mathbf{r},\mathbf{r}') \nabla_t' \cdot \mathbf{b}_n dS' dC - \int_{T_m^\pm} \nabla_t \cdot (\mathbf{b}_m \times \mathbf{n}) \int_{T_n^\pm} G_s(\mathbf{r},\mathbf{r}') \nabla_t' \cdot \mathbf{b}_n dS' dS, \quad (41)$$

where $\mathbf{l}$ is a unit vector tangent to $\partial T_m^\pm$ which has induced orientation from that of S. The second integral vanishes because $\nabla_t \cdot (\mathbf{b}_m \times \mathbf{n}) = 0$ holds for RWG functions. This implies that Galerkin's method with RWG functions as test functions may not be the most accurate discretization scheme for the Müller formulation. This has been analyzed in [53], where the use of the rotated Buffa-Christiansen functions are suggested as test functions. For our purposes, however, the results are sufficiently accurate. Thus

$$I = \int_{\partial T_m^\pm} \mathbf{b}_m \cdot \mathbf{l} \int_{T_n^\pm} G_s(\mathbf{r},\mathbf{r}') \nabla_t' \cdot \mathbf{b}_n dS' dC. \quad (42)$$

The combined kernel G_s is a continuous function due to the cancellation of $1/R$ terms.

The approximate form of the eigenvalue problem becomes

$$(\mathrm{I} + \mathrm{B}'^{-1}\mathrm{A})\mathbf{x}_n = \lambda_n \mathbf{x}_n. \quad (43)$$

The resonances occur when $\det(\mathrm{I} + \mathrm{B}'^{-1}\mathrm{A}(\omega)) = 0$ holds. The Fredholm property of $\mathcal{I} + \mathcal{A}$ guarantees that if the approximate operator converges towards the original operator with respect to some discretization parameter, then the approximate resonance frequencies also approach the exact resonance frequencies [45].

Usually electromagnetic scattering can be formulated in Lipschitz continuous domains, which allow for sharp corners, but prevent such sharpness that would lead to infinite energy in finite volumes. Being able to allow sharp features is useful, as most numerical schemes consider flat polygonal representations of the boundary surface. However, while the compactness of the operator $\mathcal{A}$ has been established for smooth surfaces, the compactness with a Lipschitz continuous surface is an open issue. Thus an additional spectral structure may be present in the numerical solutions if polygonal surfaces are used. In the approximate context, the matrix representation of the operator has as many eigenvalues as is the dimension of the matrix. Some of the eigenvalues may be related to the additional spectral structure introduced by the numerical scheme.

B. Matrix of adjoint operator

To obtain the modal expansion coefficients, we wish to obtain approximations for the adjoint modes $\mathbf{h}_n$ in the RWG basis. We can use the matrix A for this instead of finding out explicitly what $\mathcal{A}^\dagger$ is.

Let us have an operator $\mathcal{A} : H \to H$ and a basis $H_b = \{\mathbf{b}_1, \ldots, \mathbf{b}_N\}$ in a finite-dimensional subspace of H. The operator has an approximate matrix representation A in this basis, so that $A_{mn} = \langle \mathbf{b}_m, \mathcal{A}\mathbf{b}_n \rangle$. The approximate matrix representation of the adjoint operator $\mathcal{A}^\dagger$ in basis H_b is

$$\mathrm{A}^\dagger = \mathrm{B}^{-1}\mathrm{A}^*\mathrm{B}, \quad (44)$$

where $B_{mn} = \langle \mathbf{b}_m, \mathbf{b}_n \rangle$ holds and A^* is the Hermitian transpose of A. The dual basis is defined by $\langle \mathbf{b}^m, \mathbf{b}_n \rangle = \delta_{mn}$. The B matrices correspond to change from the dual basis $H^b = \{\mathbf{b}^1, \ldots, \mathbf{b}^N\}$ to the primary basis H_b.

C. Evaluation of excitation coefficients

Next, we elaborate on the evaluation of the modal excitation coefficients in the approximate context. Let us expand $\mathbf{f}$ in terms of the eigenmodes as in Eq. (26). Then, in the case of no degeneracy,

$$\alpha_n = \frac{\langle \mathbf{h}_n, \mathbf{g} \rangle}{\lambda_n \langle \mathbf{h}_n, \mathbf{f}_n \rangle} \quad (45)$$

are the coefficients for the solution to the problem $(\mathcal{I} + \mathcal{A})\mathbf{f} = \mathbf{g}$.

Let $\mathbf{h}_n$ be expanded in the RWG basis as

$$\mathbf{h}_n = \sum_m \left(a_m^{h,n} \mathbf{b}_m, b_m^{h,n} \mathbf{b}_m \right). \quad (46)$$

Then

$$\langle \mathbf{h}_n, \mathbf{g} \rangle = \sum_m \left(a_m^{h,n*} c_m^J + b_m^{h,n*} c_m^M \right), \quad (47)$$

where

$$c_m^J = 2\eta_1 \mu_1 \xi_\mu \int_S \mathbf{b}_m \cdot \mathbf{J}_{\mathrm{inc}} dS, \quad (48)$$

$$c_m^M = 2\epsilon_1 \xi_\epsilon \int_S \mathbf{b}_m \cdot \mathbf{M}_{\mathrm{inc}} dS. \quad (49)$$

The coefficients $c_m^{J/M}$ are the excitation coefficients of the vector $\mathbf{y}$ used in the approximate solution of the direct scattering problem for a given excitation source [Eq. (39)]. Thus the summation in Eq. (47) represents the projection of these coefficients to specific modes with index n.

Expand $\mathbf{f}_n$ as

$$\mathbf{f}_n = \sum_m \left(a_m^{f,n} \mathbf{b}_m, b_m^{f,n} \mathbf{b}_m \right). \quad (50)$$

Then the product $\langle \mathbf{h}_n, \mathbf{f}_n \rangle$ can be written as

$$\langle \mathbf{h}_n, \mathbf{f}_n \rangle = \sum_m \sum_{m'} \left(a_m^{h,n*} a_{m'}^{f,n} + b_m^{h,n*} b_{m'}^{f,n} \right) B_{mm'}. \quad (51)$$

To summarize, the expansion coefficients α_n can be evaluated by the use of Eqs. (47) and (51).

VI. SPHERICAL GEOMETRY: CONNECTION TO MIE THEORY

A. Theory

As an important example, we consider spherical particles. This case can also be analyzed by the Mie theory, where the internal and scattered fields are sought by the separation of variables [47]. This leads to the expansion of the fields in terms of transverse-electric (TE) and transverse-magnetic (TM) multipoles and the resonances arise from the poles of the

expansion coefficients [47]. For boundary integral operators, the solution $\mathbf{f}$ is given in terms of tangential traces of the multipoles over S [54].

In this section, we assume that the surface S of the particle is a sphere of radius a. The surface current densities can be expressed in an orthogonal basis of the Hilbert space $L^2(S)$ spanned by functions $\nabla_t Y_{lm}$ and $\mathbf{n}\times\nabla_t Y_{lm}$, where Y_{lm} are the spherical harmonics. The following properties have been discovered [54]:

$$\mathcal{D}_i \nabla_t Y_{lm} = \alpha_{il}\nabla_t Y_{lm}, \tag{52}$$

$$\mathcal{D}_i \mathbf{n}\times\nabla_t Y_{lm} = \beta_{il}\mathbf{n}\times\nabla_t Y_{lm}, \tag{53}$$

$$\mathcal{K}_i \nabla_t Y_{lm} = \gamma_{il}\mathbf{n}\times\nabla_t Y_{lm}, \tag{54}$$

$$\mathcal{K}_i \mathbf{n}\times\nabla_t Y_{lm} = \gamma_{il}\nabla_t Y_{lm}, \tag{55}$$

where

$$\alpha_{il} = \eta_i \psi_l'(x_i)\xi_l'(x_i), \tag{56}$$

$$\beta_{il} = \eta_i \psi_l(x_i)\xi_l(x_i), \tag{57}$$

$$\gamma_{il} = -i/2[\psi_l(x_i)\xi_l'(x_i) + \xi_l(x_i)\psi_l'(x_i)], \tag{58}$$

where $x_i = k_i a$ and ψ_l,ξ_l are Riccati-Bessel functions [47]. We also define $x = k_1 a$ and $Nx = k_2 a$, where $N = k_2/k_1$ is the relative index of refraction. Thus the vector spherical harmonics are eigenfunctions of $\mathcal{D}_i$ and $\mathbf{n}\times\mathcal{K}_i$.

The expansion of the solution in spherical harmonics is

$$\mathbf{f} = \sum_{l=1}^{\infty}\sum_{m=-l}^{l}(a_{lm}\nabla_t Y_{lm} + b_{lm}\mathbf{n}\times\nabla_t Y_{lm}, \\ c_{lm}\nabla_t Y_{lm} + d_{lm}\mathbf{n}\times\nabla_t Y_{lm}). \tag{59}$$

We seek transverse-electric and transverse-magnetic modes of the form

$$\mathbf{f}_{lm}^{\mathrm{TE}} = (a_l\mathbf{n}\times\nabla_t Y_{lm}, b_l\nabla_t Y_{lm}), \tag{60}$$

$$\mathbf{f}_{lm}^{\mathrm{TM}} = (a_l\nabla_t Y_{lm}, b_l\mathbf{n}\times\nabla_t Y_{lm}). \tag{61}$$

The transversality is apparent from $\nabla_t\cdot\mathbf{J} = i\omega\epsilon_1\mathbf{n}\cdot\mathbf{E}_1$, $\nabla_t\cdot\mathbf{M} = i\omega\mu_1\mathbf{n}\cdot\mathbf{H}_1$, and that $\nabla_t\cdot(\mathbf{n}\times\nabla_t\phi) = 0$ holds for all ϕ.

Operating with $\mathcal{A}$ on the TE field gives rise to the eigenvalue problem $\mathrm{A}\mathbf{x} = \chi\mathbf{x}$, where $\mathbf{x} = (a_l, b_l)^T$ and

$$\mathrm{A} = 2\begin{pmatrix} \xi_\mu(\mu_1\gamma_{1l} - \mu_2\gamma_{2l}) & \xi_\mu(-\epsilon_1\alpha_{1l} + \epsilon_2\alpha_{2l}) \\ \xi_\epsilon(-\epsilon_1\beta_{1l} + \epsilon_2\beta_{2l}) & \xi_\epsilon(-\epsilon_1\gamma_{1l} + \epsilon_2\gamma_{2l}) \end{pmatrix}. \tag{62}$$

The transverse-magnetic fields give rise to a similar eigenvalue problem with matrix

$$\mathrm{A} = 2\begin{pmatrix} \xi_\mu(-\mu_1\gamma_{1l} + \mu_2\gamma_{2l}) & \xi_\mu(-\epsilon_1\beta_{1l} + \epsilon_2\beta_{2l}) \\ \xi_\epsilon(\epsilon_1\alpha_{1l} - \epsilon_2\alpha_{2l}) & \xi_\epsilon(\epsilon_1\gamma_{1l} - \epsilon_2\gamma_{2l}) \end{pmatrix}. \tag{63}$$

Note that a 2×2 matrix always has exactly two eigenvalues, which we do not indicate explicitly in χ. A Müller eigenvalue is then given as $\lambda = 1 + \chi$. Thus we get two eigenvalues for each l in the multipole formalism. This is most likely a manifestation of the fact that the resonance frequencies appear as pairs symmetric with respect to the imaginary axis. Complex resonance frequencies ω_n, which are poles of the inverse operator, are found by solving $\det(\mathrm{I} + \mathrm{A}(\omega_n)) = 0$. Even for a sphere this procedure is iterative by nature.

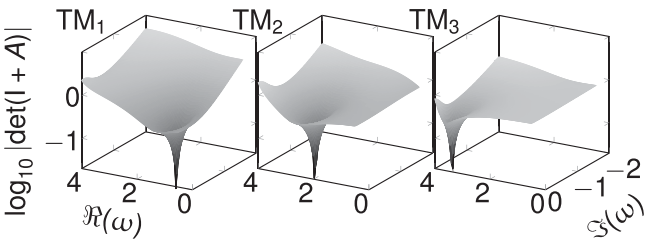

FIG. 3. Plot of the function $\log_{10}|\mathrm{I} + \mathrm{A}(\omega)|$ at complex frequencies for a gold sphere with radius 200 nm. The first three TM modes with $l = 1,2,3$ are considered.

In conclusion, we have the following results:

$$(\mathcal{I} + \mathcal{A})\,\mathbf{f}_{lm}^{\mathrm{TE}} = \lambda_l^{\mathrm{TE}}\mathbf{f}_{lm}^{\mathrm{TE}}, \tag{64}$$

$$(\mathcal{I} + \mathcal{A})\,\mathbf{f}_{lm}^{\mathrm{TM}} = \lambda_l^{\mathrm{TM}}\mathbf{f}_{lm}^{\mathrm{TM}}, \tag{65}$$

i.e., the TE and TM multipolar modes $\mathbf{f}_{lm}^{\mathrm{TE}}$ and $\mathbf{f}_{lm}^{\mathrm{TM}}$ are eigensolutions of Eq. (25). This rigorously links our general theory of modes and resonances to the traditional Mie theory.

B. Results

Consider a gold sphere of radius 200 nm in vacuum. The complex resonance frequencies defined by Eq. (23) can be found with our numerical method. For complex frequencies, we use the Drude model for the permittivity of gold with parameters obtained from fit [55]. Our method shows that the TM modes of order $l = 1,2,3$ are the most important, with resonance frequencies of $\omega_1 = 1.34 - i0.66$ PHz, $\omega_2 = 2.72 - i0.66$ PHz, and $\omega_3 = 3.68 - i0.27$ PHz. These frequencies match the nulls of the respective denominators of the traditional Mie theory, illustrating that Eq. (23) is compatible with it. In Fig. 3 we plot the quantity $\log_{10}|\det(\mathrm{I} + \mathrm{A}(\omega))|$ to illustrate how the poles of the inverse operator occur in our boundary integral approach.

We stress that these resonances were obtained without specifying any incident field. Next we compare these results to the traditional approach that uses an incident probe field. We calculate the extinction spectrum and field enhancement of the sphere for linearly polarized, incident plane-wave and measured permittivity data [56]. The results shown in Fig. 4 are typical for a large sphere: we see a very broad dipole resonance ($l = 1$) and two relatively narrow peaks corresponding to quadrupole ($l = 2$) and octupole ($l = 3$) TM modes. Extinction and field enhancement peaks occur at notably different frequencies, as known for large particles [57]. The frequencies from our theory fall between the ones obtained from extinction and field enhancement. Thus neither

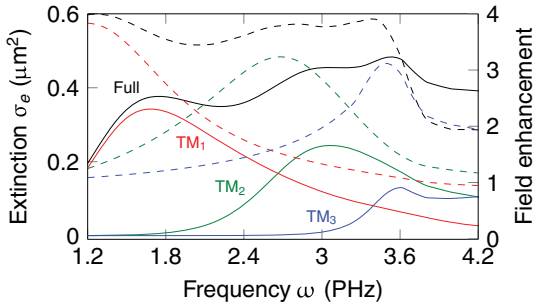

FIG. 4. (Color online) Extinction cross section (solid) and field enhancement (dashed) of a gold sphere with radius 200 nm for a linearly polarized incident plane wave. TM contributions are plotted separately from the full-wave case.

the peaks in extinction nor the peaks in field enhancement should be used to define resonance frequencies.

Next we analyze the eigenvalue spectrum defined by Eq. (25) at a real frequency $\omega = 1.7$ PHz, shown in Fig. 5. We use the analytical equations (64) and (65) and the numerical method of moments applied to Eq. (25) to validate the latter. The eigenvalues computed by the two approaches agree well. The smallest eigenvalues, making possible strong excitation, correspond to the lowest-order modes. Interestingly, the extinction of plane wave is highest due to the dipole mode (TM_1), even though its eigenvalue is not the smallest. In addition, the TM_2 mode is barely excited in spite of its small eigenvalue. This is possible because coefficients α_n also depend on $\langle \mathbf{h}_n, \mathbf{g} \rangle$, which depends on the form of excitation. Thus the modal approach implies that generally TM_2 has a stronger response than TM_1, but a plane wave is not optimal for its excitation. Lastly, we clearly observe that the eigenvalues accumulate towards the value 1, which follows directly from the compactness of $\mathcal{A}(\omega)$, as was discussed in Sec. III.

VII. RESONANCES AND MODES OF NONSPHERICAL PARTICLES

The results for the sphere shown in Fig. 4 illustrate that it is very difficult to distinguish individual modes in the extinction

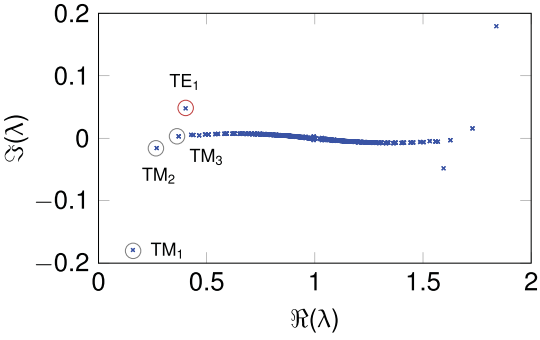

FIG. 5. (Color online) Eigenvalues of I + A at frequency 1.7 PHz for a gold sphere of radius 200 nm. Dots are calculated by method of moments and circles by analytic theory.

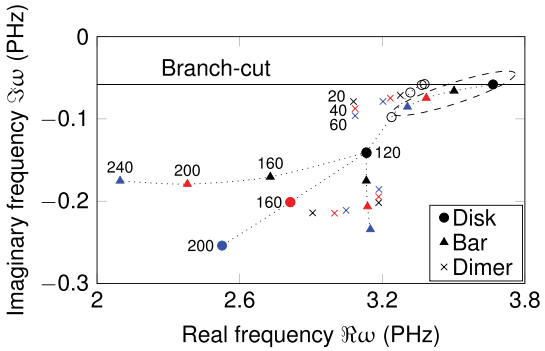

FIG. 6. (Color online) Resonance frequencies in the complex frequency plane. Numbers and colors indicate the varied parameter of particular structure. Dotted lines illustrate the trends in resonance shifts. The degenerate resonance of the disk clearly splits into branches for the bar and dimer. Circles correspond to a down-scaled disk that approaches the quasistatic limit, whence the resonances approach the branch cut. The encircled marks correspond to higher-order resonances.

spectrum. For spherical particles, we can resort to the multipole expansion, but without our modal theory this is impossible in other geometries. We next demonstrate the power of our approach, without any assumed incident field, by considering prototypical nonspherical structures. We consider three flat gold nanostructures: a circular disk, a disk dimer, and a bar, all with gold thickness of 20 nm. For the disk, we consider the diameters of 120, 160, and 200 nm. For the dimer, we consider the diameter of 120 nm and gap sizes of 20, 40, and 60 nm. For the bar, we consider the width of 120 nm and lengths of 160, 200, and 240 nm.

We utilize the Drude model again to find the complex resonance frequencies of the structures, which are shown in Fig. 6. The resonances exhibit intuitive behavior: increasing particle size or aspect ratio shifts the real part of resonance frequency $\Re\omega_n$ to lower values. The disk resonance is degenerate, but stretching it into a bar splits the resonance into two branches, related to plasmon oscillations along two directions. For the dimer, the degenerate resonances of the two disks produce four branches. This is thus an exact electromagnetic treatment of "mode hybridization" [6,7]. Notice that the resonance frequencies are off the branch cut, where the resonance frequencies are predicted to reside by the quasistatic theory. This emphasizes the importance of radiative effects.

Next we discuss the modes and corresponding radiation patterns, calculated numerically from Eq. (25), at real frequencies close to the complex resonance frequencies of Fig. 6. At each fixed frequency, there is a discrete set of modes, but we only consider a few of those corresponding to lowest-in-magnitude eigenvalues.

In Fig. 7 the modes of the disk of diameter 120 nm at frequency 3.14 PHz are shown. Note that the charge densities for all modes are normalized between -1 and $+1$, as the eigenmodes as such do not have any inherent strength. The first two modes are the typical dipole modes, which are degenerate due to the rotational symmetry. Here the term "dipole mode" is defined rigorously without relying on the multipole theory,

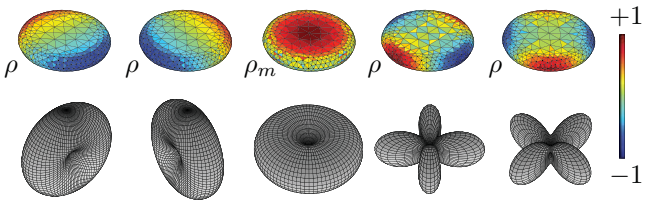

FIG. 7. (Color online) Mode charge densities and radiation patterns at fixed real frequency 3.14 PHz for the gold nanodisk of diameter 120 nm. The charge densities correspond to a time instant of harmonic oscillation and are normalized to unity.

which is strictly defined only for spherical particles. These are plasmon modes that are characterized by accumulating electric surface charge $\rho = \epsilon_0 \mathbf{n} \cdot \mathbf{E}_1$. For the third mode, however, the accumulating quantity is the equivalent surface magnetic charge $\rho_m = \mu_0 \mathbf{n} \cdot \mathbf{H}_1$. Such modes are due to eddy currents and are analogous to TE modes of the sphere. It would be difficult to find such responses by a plane-wave probe field due to polarization mismatch and simultaneous excitation of other modes. The last two modes are again degenerate plasmon modes, but of higher order.

Figure 8 shows the modes of the dimer of gap length 20 nm at frequency 3.14 PHz. The first two modes of the top row are the "dark" hybridized plasmon modes with no radiation along the disk axis. The third mode of the top row and the first mode of the bottom row are the "bright" hybridized plasmon modes. The last two modes of the bottom row are hybridized eddy current, i.e., magnetic modes.

The modes of the bar of length 200 nm at frequency 2.38 PHz are shown in Fig. 9. The first two modes of the top row are the plasmon modes related to oscillation of electrons along the length and width of the bar, respectively. The third mode of the top row is a magnetic mode. The three modes in the bottom row are higher-order plasmon modes, the first two being "dark" and the last being "bright."

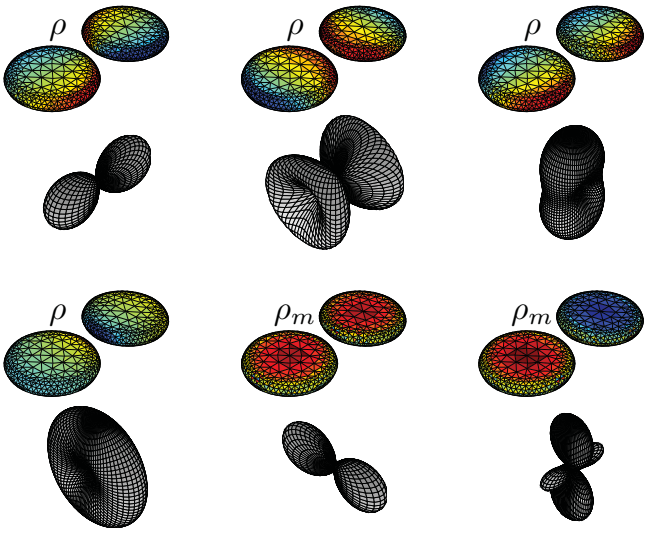

FIG. 8. (Color online) Mode charge densities and radiation patterns at fixed real frequency 3.14 PHz for the gold nanodisk dimer of gap length 20 nm. The color scale is that of Fig. 7.

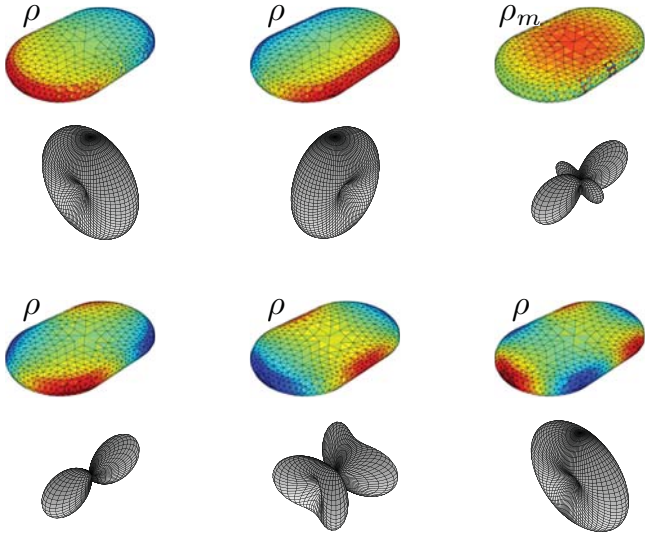

FIG. 9. (Color online) Mode charge densities and radiation patterns at fixed real frequency 2.38 PHz for the gold nanobar dimer of length 200 nm. The color scale is that of Fig. 7.

VIII. DISCUSSION

We now turn to more subtle aspects of our approach. The solution space over S is *separable*, and thus it has a discrete basis (the so-called Schauder basis) [58]. However, it is not yet proven that the eigenmodes $\mathbf{f}_n$ constitute such basis. Nevertheless, we have verified that only a few modes are required to describe typical excited solutions very accurately.

The reason why one obtains an eigenbasis for cavity resonator and waveguide problems is that the governing operator is compact and self-adjoint. The operator K in the quasistatic scattering theory, introduced in Sec. IV B, is also compact and self-adjoint with respect to a certain inner product, which is closely related to energy [59]. In the full-wave scattering problem, the corresponding operator is compact in the Müller formulation, but it is not self-adjoint. The reason for this is that, in the full-wave case, the Green's function is complex valued due to the factor $\exp(ikR)$ as opposed to the static case. This is true for the inner product defined in Eq. (22), but that this is true for any other inner product as well is suggested by the fact that, even for the sphere, the eigenvalues are complex numbers. A prior study of modes for dielectric scatterers considered the PMCHWT formulation, from which a generalized eigenvalue problem was derived [38]. The pertinent operators were pseudo-self-adjoint by construction, but not compact. Thus the full-wave scattering problem may not admit a description by a compact self-adjoint operator.

On the other hand, a discrete basis can be found in the Müller formulation: The Riesz-Schauder theory states that a compact operator has a *singular value decomposition* (SVD) [58]. Thus the range of our operator $\mathcal{A}$ may be rigorously

expanded as

$$\mathcal{A}\mathbf{f} = \sum_{n=1}^{\infty} s_n \langle \mathbf{f}, \mathbf{x}_n \rangle \mathbf{y}_n, \tag{66}$$

where $\mathcal{A}^\dagger \mathcal{A}\mathbf{x}_n = s_n^2 \mathbf{x}_n$ and $\mathcal{A}\mathcal{A}^\dagger \mathbf{y}_n = s_n^2 \mathbf{y}_n$ hold and the numbers s_n are called the singular values. These composite operators are compact because $\mathcal{A}$ is compact, and they are also self-adjoint by construction. Unfortunately, our current understanding is that the singular values s_n are not strictly related to the resonances given by Eq. (23).

The modes and resonances of scatterers have been studied by various integral operator approaches, especially for perfectly conducting bodies. It is interesting how the different formulations lead to different operator properties, allowing resonances to be rigorously identified in one formulation but not in the other. We believe that the resonances, as defined by Eq. (23), are the true physical resonances and any other formulation of the scattering problem should be able to find these. Other formulations may predict additional nonphysical resonances, which is known to happen for, e.g., the electric field integral equation (EFIE) and magnetic field integral equation (MFIE) formulations [49].

As we discussed above, even in the Müller formulation, we may define modes in several ways: as eigenfunctions of the operator $\mathcal{I} + \mathcal{A}(\omega)$ at fixed real frequency, as eigenfunctions $\mathbf{f}_{0n}$ corresponding to the complex resonance frequencies ω_n by $(\mathcal{I} + \mathcal{A}(\omega_n))\mathbf{f}_{0n}$, or as eigenfunctions $\mathbf{y}_n$ appearing in the SVD for a fixed real frequency. On the other hand, in, e.g., the volume integral operator formulation, the domain of the eigenfunctions is the volume of the particle as opposed to the surface in the boundary integral formulation. It is not clear whether these modes map to each other in a trivial way. We feel that understanding the relation between different mode definitions is an open issue that should be investigated in the future.

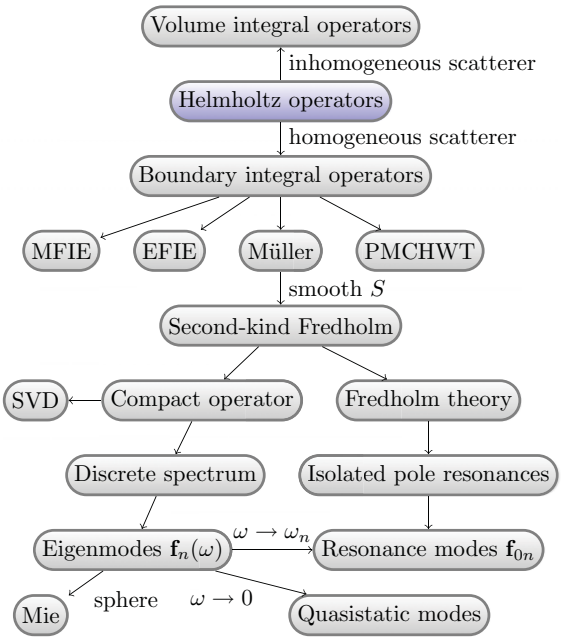

FIG. 10. (Color online) Diagram of the strategy towards the definition of modes and resonances in scattering problems by boundary integral operators.

The various formulations of the scattering problem are illustrated in Fig. 10. For the boundary integral approach, various formulations exist and only a few of them are listed. We emphasize that the Müller formulation leads to theoretically the most rigorous approach to the definition of modes and resonances.

IX. CONCLUSION

We have successfully defined modes and resonances for dielectric and plasmonic scatterers by the use of boundary integral operators in a full-wave approach. We concluded that the Müller formulation admits a rigorous definition of the resonances as properties of the scatterer by relying on the second-kind Fredholm property of the pertinent boundary integral operator. The Fredholm theory allowed us to establish that the resonance frequencies are isolated points in the complex plane, and any other singularities are the possible branch cuts from the material dispersion relation. We further proposed an expansion of solutions with respect to eigenmodes, which are independent of incident field and defined at fixed real frequencies. The second-kind Fredholm property guaranteed the discreteness of the modal expansion as well.

The modes and resonances were connected to the traditional Mie theory in the case of spherical particles. This was accomplished by proving that the boundary restrictions of the multipole fields are eigenfunctions of the considered boundary integral operator. We also showed that the general definition of modes naturally reduced to the earlier quasistatic definitions in the limit of zero frequency.

We presented illustrative examples for the sphere and for nonspherical flat gold nanostructures. The resonance frequencies were found to obey intuitive shifting and splitting behaviors as the geometrical parameters were varied. The near fields and radiation patterns of the corresponding modes at real frequencies were presented and analyzed. The modes were characterized as bright or dark modes and further classified as plasmon or eddy current modes.

In conclusion, our theory provides a unifying framework for the analysis of resonances as well as near and far fields in scattering problems. The approach reveals the important physics of scattering systems directly and can fundamentally change the way these systems are optimized and understood. The present paper has considered plasmonic systems as an example of particular interest. However, the approach is applicable to any material describable by complex permittivity and permeability. Such materials are constantly emerging for nanophotonic applications.

ACKNOWLEDGMENTS

The authors thank Prof. Ralf Hiptmair for assistance with the integral operator theory and Dr. Pasi Ylä-Oijala for helpful advice regarding boundary integral operators. J.M. acknowledges the graduate school of Tampere University of Technology for funding.

[1] U. Kreibig and M. Vollmer, *Optical Properties of Metal Clusters* (Springer-Verlag, Berlin, 1995).

[2] J. Jackson, S. Westcott, L. Hirsch, J. West, and N. Halas, Appl. Phys. Lett. **82**, 257 (2003).

[3] K. Li, M. I. Stockman, and D. J. Bergman, Phys. Rev. B **72**, 153401 (2005).

[4] K. L. Kelly, E. Coronado, L. L. Zhao, and G. C. Schatz, J. Phys. Chem. B **107**, 668 (2003).

[5] M.-W. Chu, V. Myroshnychenko, C. H. Chen, J.-P. Deng, C.-Y. Mou, and F. J. García de Abajo, Nano Lett. **9**, 399 (2008).

[6] E. Prodan, C. Radloff, N. J. Halas, and P. Nordlander, Science **302**, 419 (2003).

[7] P. Nordlander, C. Oubre, E. Prodan, K. Li, and M. Stockman, Nano Lett. **4**, 899 (2004).

[8] D. R. Fredkin and I. D. Mayergoyz, Phys. Rev. Lett. **91**, 253902 (2003).

[9] I. D. Mayergoyz, D. R. Fredkin, and Z. Zhang, Phys. Rev. B **72**, 155412 (2005).

[10] D. E. Gomez, K. C. Vernon, and T. J. Davis, Phys. Rev. B **81**, 075414 (2010).

[11] K. Li, M. I. Stockman, and D. J. Bergman, Phys. Rev. Lett. **91**, 227402 (2003).

[12] M. I. Stockman, S. V. Faleev, and D. J. Bergman, Phys. Rev. Lett. **87**, 167401 (2001).

[13] C. E. Baum, On the Singularity Expansion Method for the Solution of Electromagnetic Interaction Problems, Tech. Rep., DTIC Document, 1971 (unpublished), http://www.dtic.mil/docs/citations/ADA066905.

[14] R. Garbacz and R. Turpin, IEEE Trans. Antennas Propag. **19**, 348 (1971).

[15] R. Harrington and J. Mautz, IEEE Trans. Antennas Propag. **19**, 622 (1971).

[16] R. Harrington and J. Mautz, IEEE Trans. Antennas Propag. **19**, 629 (1971).

[17] M. Capek, P. Hazdra, and J. Eichler, IEEE Trans. Antennas Propag. **60**, 4556 (2012).

[18] R. Harrington, J. Mautz, and Y. Chang, IEEE Trans. Antennas Propag. **20**, 194 (1972).

[19] D. J. Bergman and D. Stroud, Phys. Rev. B **22**, 3527 (1980).

[20] G. Hanson and C. Baum, Interaction Note 517 (1996), http://www.ece.unm.edu/summa/notes/Interaction.html.

[21] J. R. de Lasson, J. Mørk, and P. T. Kristensen, J. Opt. Soc. Am. B **30**, 1996 (2013).

[22] X. Zheng, V. Volskiy, V. K. Valev, G. A. Vandenbosch, and V. V. Moshchalkov, IEEE J. Sel. Top. Quantum Electron. **19**, 4600908 (2013).

[23] X. Zheng, N. Verellen, V. Volskiy, V. K. Valev, J. J. Baumberg, G. A. Vandenbosch, and V. V. Moshchalkov, Opt. Express **21**, 31105 (2013).

[24] N. Budko and A. Samokhin, SIAM J. Sci. Comp. **28**, 682 (2006).

[25] N. V. Budko and A. B. Samokhin, Phys. Rev. Lett. **96**, 023904 (2006).

[26] Y. Zhou, Ph.D. thesis, Harvard University, 2010.

[27] V. A. Markel, J. Opt. Soc. Am. B **12**, 1783 (1995).

[28] N. A. Gippius, T. Weiss, S. G. Tikhodeev, and H. Giessen, Opt. Express **18**, 7569 (2010).

[29] T. Weiss, N. Gippius, S. Tikhodeev, G. Granet, and H. Giessen, J. Opt. Soc. Am. A **28**, 238 (2011).

[30] H. Guo, B. Oswald, and P. Arbenz, Opt. Express **20**, 5481 (2012).

[31] Q. Bai, M. Perrin, C. Sauvan, J.-P. Hugonin, and P. Lalanne, Opt. Express **21**, 27371 (2013).

[32] F. J. de Abajo and A. Howie, Phys. Rev. B **65**, 115418 (2002).

[33] G. W. Bryant, F. J. García de Abajo, and J. Aizpurua, Nano Lett. **8**, 631 (2008).

[34] A. M. Kern and O. J. Martin, J. Opt. Soc. Am. A **26**, 732 (2009).

[35] C. Forestiere, G. Iadarola, G. Rubinacci, A. Tamburrino, L. Dal Negro, and G. Miano, J. Opt. Soc. Am. A **29**, 2314 (2012).

[36] J. Mäkitalo, S. Suuriniemi, and M. Kauranen, Opt. Express **19**, 23386 (2011).

[37] P. Heider, Comput. Math. Appl. **60**, 1620 (2010).

[38] Y. Chang and R. Harrington, IEEE Trans. Antennas Propag. **25**, 789 (1977).

[39] C. Sauvan, J.-P. Hugonin, I. S. Maksymov, and P. Lalanne, Phys. Rev. Lett. **110**, 237401 (2013).

[40] P. T. Kristensen and S. Hughes, ACS Photonics **1**, 2 (2014).

[41] L. Novotny and B. Hecht, *Principles of Nano-optics* (Cambridge University Press, Cambridge, UK, 2006).

[42] J. A. Stratton, *Electromagnetic Theory* (McGraw-Hill College, New York, 1941).

[43] C. Müller, *Foundations of the Mathematical Theory of Electromagnetic Waves* (Springer-Verlag, Berlin, 1969).

[44] P. Ylä-Oijala and M. Taskinen, IEEE Trans. Antennas Propag. **53**, 3316 (2005).

[45] G. W. Hanson and A. B. Yakovlev, *Operator Theory for Electromagnetics: An Introduction* (Springer, New York, 2001).

[46] S. Steinberg, Arch. Rational Mech. Anal. **31**, 372 (1968).

[47] C. F. Bohren and D. R. Huffman, *Absorption and Scattering of Light by Small Particles* (John Wiley & Sons, New York, 2008).

[48] D. Giri and F. Tesche, Electromagnetics **1**, 455 (1981).

[49] R. F. Harrington, J. Electromagnet. Wave. **3**, 1 (1989).

[50] R. F. Harrington, *Field Computation by Moment Methods* (Wiley-IEEE Press, New York, 1993).

[51] S. Rao, D. Wilton, and A. Glisson, IEEE Trans. Antennas Propag. **30**, 409 (1982).

[52] I. Hänninen, M. Taskinen, and J. Sarvas, Prog. Electromagn. Res. **63**, 243 (2006).

[53] P. Ylä-Oijala, S. Kiminki, K. Cools, F. Andriulli, and S. Järvenpää, Int. J. Numer. Model. **25**, 525 (2012).

[54] G. C. Hsiao and R. E. Kleinman, IEEE Trans. Antennas Propag. **45**, 316 (1997).

[55] A. Vial, A.-S. Grimault, D. Macías, D. Barchiesi, and M. L. de la Chapelle, Phys. Rev. B **71**, 085416 (2005).

[56] P. B. Johnson and R. Christy, Phys. Rev. B **6**, 4370 (1972).

[57] B. M. Ross and L. P. Lee, Opt. Lett. **34**, 896 (2009).

[58] M. Reed and B. Simon, *Methods of Modern Mathematical Physics: Functional Analysis* (Gulf Professional Publishing, Houston, TX, 1980), Vol. 1.

[59] I. D. Mayergoyz, *Plasmon Resonances in Nanoparticles* (World Scientific, Singapore, 2013).